

Superfluidity and spin superfluidity in spinor Bose gases

J. Armitis*

*Institute of Theoretical Physics and Astronomy,
Vilnius University,
A. Goštauto 12, LT-01108 Vilnius, Lithuania*

R. A. Duine

*Institute for Theoretical Physics and Center for Extreme Matter and Emergent Phenomena,
Utrecht University,
Leuvenlaan 4, 3584 CE Utrecht, The Netherlands
(Dated: December 3, 2024)*

We investigate the interplay between superfluidity and spin superfluidity in spinor Bose gases with easy-plane anisotropy. To illustrate that the basic principles governing these two types of superfluidity are the same, we describe the magnetization and particle-density dynamics in a single hydrodynamic framework. In this description spin and mass supercurrents are driven by their respective chemical potential gradients. As an application, we propose an experimentally-accessible stationary state, where the two types of supercurrents counterflow and cancel each other, thus resulting in no mass transport. Furthermore, we propose a straightforward setup to probe spin superfluidity by measuring the in-plane magnetization angle of the whole cloud of atoms. We verify the robustness of these findings by evaluating the four-magnon collision time, and find that the timescale for coherent (superfluid) dynamics is separated from that of the slower incoherent dynamics by one order of magnitude. Comparing the atom and magnon kinetics reveals that while the former can be hydrodynamic, the latter is typically collisionless under most experimental conditions. This implies that, while our zero-temperature hydrodynamic equations are a valid description of spin transport in Bose gases, a hydrodynamic description that treats both mass and spin transport at finite temperatures may not be readily feasible.

PACS numbers: 03.75.Mn, 03.75.Kk, 05.30.Jp, 67.85.Fg, 85.75.-d

Introduction.— The phenomenon of superfluidity underlies transport properties of numerous systems, including various superconductors [1], liquid helium [2], both bosonic [3] and fermionic [4] ultracold atoms, exciton-polariton condensates [5], topological insulators [6–8], as well as neutron stars [9] and flocks of birds [10]. The possibility to achieve dissipationless propagation of information at room temperature has recently fueled interest in spin superfluidity [11, 12] in general and in magnon spintronics [13–15] in particular.

Ferromagnetic spinor Bose-Einstein condensates of atomic vapour stand out among these systems as a rare example where two types of superfluidity can be present simultaneously, and where they are also readily experimentally addressable. Specifically, experimental ultracold atom techniques currently allow controlled excitation and imaging of both the local phase of the condensate, and also of the spin texture. Exciting mass supercurrents (pertaining to inhomogeneity of the local phase of the wavefunction) in the system is possible by, e.g., stirring the condensate with an “optical spoon” [16]. Signatures of this mass superfluidity have been observed in the collective mode spectrum [17] and lattices of quantized vortices [18]. Furthermore, manipulating and observing the spin texture (or, equivalently, the spin supercurrent [11]) has recently also become possible in this system. In particular, spin-agnostic optical traps [19] have allowed preparation and subsequent imaging of spinor

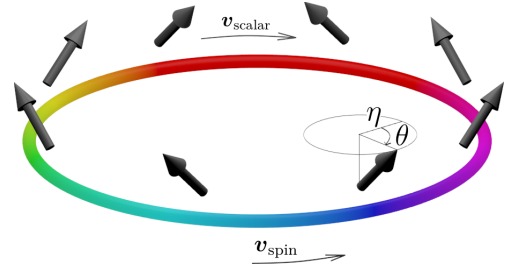


FIG. 1. By counterflowing, a supercurrent and a spin supercurrent create a stationary state with no mass flow in a spinor Bose gas on a ring. In a uniform-density system, the supercurrent $\mathbf{v}_{\text{scalar}}$ is due to the global phase texture of the atomic condensate (indicated by color), whereas the spin supercurrent \mathbf{v}_{spin} is due to the in-plane magnetization texture (indicated by arrows which can be recast in terms of a phase θ) of the magnon condensate with a measure of the condensate fraction η . The two textures can be independently engineered in a ferromagnetic spinor Bose gas.

gases, for example, using the Stern-Gerlach method [20] and also directly [21]. Several methods for imprinting spin textures have been developed, either relying on varying external magnetic fields [22] or optical transitions [23].

Earlier work [24] has investigated stability of the planar spin spiral (XY spiral), which is one of the states that we consider (Fig. 1). Both adiabatic and sudden preparation was carefully considered, and it was demon-

strated that this state is stable for sufficiently small spiral wave vectors. However, despite the recent observation of a (quasi-)condensate of magnons [25], few studies have been devoted to spin superfluidity in ultracold spinor gas [26–28], even though this phenomenon has played a prominent role in liquid helium systems [29]. Furthermore, the interplay of mass and spin superfluidity has not been addressed in the ultracold-atom context to the best of our knowledge. In this Letter we examine coherent dynamics of spinor Bose gases, concentrating on superfluidity, spin superfluidity, and their interplay. We construct a hydrodynamic model that incorporates both types of superfluidity on equal footing. In linear response, they are decoupled. We determine both the collective mode spectrum and demonstrate that spin superfluidity can be experimentally observed by monitoring the in-plane magnetization angle of the atoms. Moreover, we demonstrate that non-linear effects lead to experimentally stationary states where both supercurrents are counterflowing. Finally, we check the robustness of our findings by comparing the timescales relevant to these coherent processes with the collision timescales describing incoherent dynamics of this system and show that they are well separated.

Theoretical framework.— We consider a spinor Bose gas described by the second-quantized Hamiltonian [30–32] $\hat{H} = \hat{H}_0 + \hat{H}_Z + \hat{H}_I$, where $\hat{H}_0 = \int d\mathbf{x} \hat{\psi}_\mu^\dagger (-\hbar^2 \nabla^2 / 2M + V(\mathbf{x})) \hat{\psi}_\mu$ represents the kinetic energy and the trapping potential $V(\mathbf{x})$. The field operators $\hat{\psi}_\mu$ correspond to atoms with mass M in the hyperfine state μ . (We use the Einstein summation convention throughout the Letter.) The linear and quadratic Zeeman effects are described by $\hat{H}_Z = - \int d\mathbf{x} \hat{\psi}_\mu^\dagger (p[\sigma_z]_{\mu\nu} - \hbar K [\sigma_z^2]_{\mu\nu}) \hat{\psi}_\nu$, where p ($\hbar K$) is the energy of the linear (quadratic) Zeeman effect, and $\sigma_{\mu\nu}$ is a vector of spin matrices. The external magnetic field has been chosen to point in the z -direction. The interactions between particles are described by $\hat{H}_I = \int d\mathbf{x} (g_0 : \hat{\rho}^2 : + g_1 : \hat{\mathbf{n}}^2 :)$, where the colons denote normal ordering, g_1 (g_0) is the spin-(in)dependent interaction energy, $\hat{\rho} = \hat{\psi}_\mu^\dagger \hat{\psi}_\mu$ is the density operator, and $\hat{\mathbf{n}} = \hat{\psi}_\mu^\dagger \boldsymbol{\sigma}_{\mu\nu} \hat{\psi}_\nu / \hat{\rho}$ is the local spin operator.

The equations for $\langle \hat{\psi}_\mu \rangle$ governing the mean-field dynamics of this system at zero temperature can be derived from the Hamiltonian \hat{H} and written down in terms of a set of conserved variables. At this point we restrict ourselves to the ferromagnetic state with the saturated local magnetization $\mathbf{n}^2 = 1$, where the local magnetization is defined by $\mathbf{n} = \langle \hat{\psi}_\mu^\dagger \boldsymbol{\sigma}_{\mu\nu} \hat{\psi}_\nu / \hat{\rho} \rangle$, which implies that we do not consider the nematic [30–32] or antiferromagnetic [33] evolution. Furthermore, we do not consider the trapping potential and the quantum pressure term [3]. Moreover, we omit the linear Zeeman effect, as it can be removed by going to a rotating coordinate system. In order to write down these mean-field equations in a concise manner, we

define the usual Eulerian derivative $D_t = \partial_t + \mathbf{v} \cdot \nabla$, where the velocity $\mathbf{v} = -i(\hbar/2M)(\psi_\mu^* \nabla \psi_\mu - [\nabla \psi_\mu^*] \psi_\mu) / \rho$ governs mass transport but has contributions from both the global phase of the wavefunction and the spin texture. In particular, we find that magnetization dynamics in a ferromagnetic spinor Bose gas is described by a Landau-Lifshitz (LL) equation [34]

$$D_t \mathbf{n} = J \mathbf{n} \times \nabla^2 \mathbf{n} - K \mathbf{n} \times \mathbf{e}_z n_z + J(\mathbf{n} \times \nabla_i \mathbf{n})(\nabla_i \rho) / \rho, \quad (1)$$

where $\rho = \langle \hat{\rho} \rangle$ is the average density (at zero temperature equal to the atomic condensate density) and the exchange constant J comes from the kinetic term in \hat{H} and describes spin stiffness. Neglecting interactions between spin waves, at low temperature the spin stiffness is [35] $J = \hbar/2M$. The magnetic anisotropy comes from the quadratic Zeeman effect. It can be generated using a sufficiently strong external magnetic field, in addition to radio-frequency and optical means [31]. Three (spin-1) or more hyperfine states are required for the magnetic anisotropy to be available in an atomic system. When $K < 0$, it is favorable for the spin to align with the director of the magnetic field. In this case z is known as the easy axis. On the other hand, in the so-called easy-plane situation $K > 0$, the configuration with \mathbf{n} perpendicular to the z axis is energetically favored. Both of these situations can be achieved in a system of ultracold atoms [31]. In addition to the terms already present in the LL equation, various spin-relaxation terms may be added, such as the transverse spin diffusion [36] and Gilbert damping [37], as well as terms due to magnetic field inhomogeneities [38] and magnetic dipole-dipole interactions [39]. However, all these terms can be made small in an ultracold-atom system, hence, we do not consider them here.

Magnon condensate.— Deep in the ferromagnetic regime where the spin excitations are small deviations from the average direction of the magnetization, it is natural to describe the magnetization dynamics in terms of magnons. Going to this description requires performing the Holstein-Primakoff transformation [40], which introduces bosonic magnon operators (see *Supplemental Material* for more details). This gas of magnons can have a thermal component, and also a condensate component. The condensate of magnons [41, 42] corresponds to the coherent magnetization precession of the spins in the whole sample. The symmetry that is broken when the magnon condensate forms concerns the in-plane magnetization angle θ , and the order parameter is related to the out-of-plane magnetization component n_z .

In order to concentrate on the superfluidity in this system, we do not describe the thermal magnons, and we also do not investigate the complicated magnon condensation process [25]. Instead, we propose to start from a sample that is homogeneously magnetized in the z direction, and then coherently tilt the magnetization (e.g., by

an RF pulse) towards the $x - y$ plane. This populates the pure-magnon-condensate state directly by preparing the magnetization of the system in the following configuration:

$$\mathbf{n} = (\eta \cos \theta, \eta \sin \theta, \sqrt{1 - \eta^2}), \quad (2)$$

where $\eta = \sqrt{2\tilde{\eta}/(1 + \tilde{\eta}^2)}$ is a measure of the local magnon-condensate fraction $\tilde{\eta}$ [43], and θ is the local in-plane angle. That this magnetization configuration indeed corresponds to a magnon condensate is understood by noting that $n_x \sim \text{Re}\langle\hat{b}\rangle$ and $n_y \sim \text{Im}\langle\hat{b}\rangle$, where \hat{b} is the Holstein-Primakoff operator that annihilates a magnon.

Using Eq. (2) together with the Landau-Lifshitz equation Eq. (1), and using the mean-field equations for the total density, we obtain a set of hydrodynamic equations, governing the evolution of the magnon condensate and the scalar condensate at zero temperature:

$$D_t \rho / \rho = -\nabla \cdot \mathbf{v}, \quad M D_t \mathbf{v} = -\nabla \mu, \quad (3)$$

$$D_t n_z + \mathbf{v}_{\text{spin}} \cdot \nabla \rho / \rho = -\nabla \cdot \mathbf{v}_{\text{spin}}, \quad \hbar D_t \theta = -\mu_{\text{spin}}, \quad (4)$$

where $\mu = (g_0 + g_1)\rho + \hbar^2(\nabla n_\mu)^2/4M$, and $\mu_{\text{spin}}/\hbar J = n_z(\nabla \theta)^2 - (\nabla^2 \eta)/n_z \eta - (\nabla \eta)^2/n_z^3 - K n_z/J$ are the chemical potentials. Their gradients drive the mass and spin supercurrents. These hydrodynamic equations describe spin and mass superfluidity in a single framework, therefore constituting the central result of our Letter.

The total velocity can be separated into two parts [30], that can be addressed separately [16, 22, 23]. First, we have the conventional superfluid velocity $\mathbf{v}_{\text{scalar}} = (\hbar/M)\nabla \phi$ due to the phase ϕ texture of the atomic condensate wavefunction. However, there also is the spin superfluid velocity $\mathbf{v}_{\text{spin}} = -J\eta^2\nabla \theta$ due to the phase θ texture of the magnon condensate. Thus, the full velocity in this ferromagnetic spinor Bose condensate is $\mathbf{v} = \mathbf{v}_{\text{scalar}} + 2n_z\mathbf{v}_{\text{spin}}/\eta^2$. This velocity \mathbf{v} influences the magnetization dynamics through the advection term in the Eulerian derivative since the magnetic moments (individual atoms) are mobile in a cold-atom system, similarly to e.g. so-called ferromagnetic superconductors [44]. This is in contrast to most solid-state ferromagnets, where the magnetic moments are localized.

Collective modes.— In the linear regime, the two superfluids are decoupled as the Eulerian derivatives become ordinary derivatives. The elementary excitations in the homogeneous magnon condensate ($\eta, \theta = \text{const.}$) have a dispersion

$$\omega^2 = KJ\eta^2k^2 + J^2k^4, \quad (5)$$

which follows from the equations of motion above. Moreover, the dispersion of the density excitations follow the Bogoliubov dispersion,

$$\omega^2 = (\hbar/2M)k^2[(\hbar/2M)k^2 + 2(g_0 + g_1)\rho/\hbar]. \quad (6)$$

At long wavelengths the dispersion is linear in both cases, with the speed of sound equal to $c_{\text{spin}} = \sqrt{KJ\eta^2}$ for the

spin excitations and $c_{\text{scalar}} = \sqrt{(g_0 + g_1)\rho/m}$ for the density excitations, signaling that we are dealing with a superfluid, as using the Landau argument [45] one can show that excitations travelling with velocities slower than the lower of these two speeds of sound are not damped. From this point on we only consider the critical spin superfluid velocity and drop its subscript: $c \equiv c_{\text{spin}}$. Note that this homogeneous state is stable and displays spin superfluidity in the easy-plane situation $K > 0$ only.

In order to verify that the system is indeed a spin superfluid and to show that the conventional superfluidity and the spin superfluidity stand on an equal footing, we propose two experiments which should be realizable with current experimental techniques. To keep the description as simple as possible, we work in the one-dimensional limit, where the spatial confinement is strong in two dimensions and more gentle in the remaining spatial dimension. Furthermore, in order to avoid complications due to trap averaging, we consider a box trap [46].

Far-from-equilibrium spin superfluidity signature.— One of the hallmarks of superfluidity is an unobstructed flow of current. In particular, in a spin superfluid, a spin current can flow with no dissipation as opposed to a system with diffusive spin transport [47], where the spin current decays after traversing some finite length, which depends on the diffusion length and on the timescales of various spin relaxation mechanisms [11]. In this section we describe a stationary state (Fig. 1) where the supercurrent and the spin supercurrent flow in opposite directions, resulting in no mass transport. However, since the spin current flows through the whole sample, it thus illustrates dissipationless spin transport [11].

By considering linear gradients in the atomic condensate phase ϕ and in the magnon condensate phase θ with a constant magnon condensate fraction η , from Eqs. (4) we find the stationary-state condition

$$\phi' = \frac{n_z}{2} \left(\theta' + \frac{K}{J\theta'} \right), \quad (7)$$

where the primes indicate spatial derivatives. In order to show that this condition can be satisfied for realistic experimental parameters, we consider a concrete example of a ring of length L filled with a cloud of spin-1 atoms (e.g. the $F = 1$ hyperfine manifold of ^{87}Rb) prepared in the magnon-condensate state described by Eq. (2). In that case, a state with $n_z = 1/2$ where the atomic condensate phase winds once ($\phi' = 2\pi/L$), while the magnon condensate phase has two windings ($\theta' = 2 \times 2\pi/L$), is stationary for $KL^2/\pi^2J = 16$. For a ring of length $L = 12\mu\text{m}$, we have $J\pi^2/L^2 \simeq 25\text{Hz}$, which requires a moderate easy-axis anisotropy of 400Hz. Moreover, this static state implies no mass transport as $\mathbf{v}_{\text{scalar}}$ exactly cancels \mathbf{v}_{spin} , and thus $\mathbf{v} = 0$. Note that without easy-plane anisotropy, and therefore without spin superfluidity, such steady states cannot be obtained.

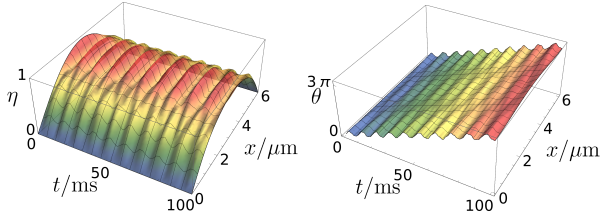


FIG. 2. Evolution of a sine-shaped magnon condensate packet for realistic experimental parameters: an $L = 6\mu\text{m}$ -long cloud of ^{87}Rb atoms, with the resulting exchange $J\pi^2/L^2 \simeq 100\text{Hz}$, easy-plane anisotropy of $K = 300\text{Hz}$, and a peak initial condensate density of $\eta_0 = 0.95$. The density of the condensate η (left) is almost unaffected by the dynamics, while the in-plane angle θ (right) evolves almost uniformly (see text for more details). The in-plane magnetization completes a full rotation in approximately 60ms. Note that the total magnetization in the z direction is conserved during the evolution.

Close-to-equilibrium spin superfluidity signature.— It is also possible to observe a signature of spin superfluidity by measuring the time evolution of the in-plane magnetization angle θ in the simple “bar” geometry (as opposed to the ring discussed above). To that end, consider a magnon condensate with a constant atomic condensate phase ϕ and a constant in-plane angle θ , in addition to a smoothly varying magnon condensate fraction bump $\eta = \eta_0 \sin(\pi x/L)$ at the initial time $t = 0$, where L is the length of the atomic cloud and x is the spatial coordinate. In this case, up to the lowest order in the gradient expansion, the time evolution preserves the magnon-condensate-density profile such that $\partial_t \eta = 0$, while the in-plane angle rotates in time with no spatial profile developing,

$$\partial_t \theta = K \langle n_z \rangle - J\pi^2 / \langle n_z \rangle L^2, \quad (8)$$

where $\langle n_z \rangle = 2\mathcal{E}[\eta_0^2]/\pi$ is the z component of magnetization averaged over the length of the cloud, and \mathcal{E} is the complete elliptic integral.

A system with a linear dispersion can only be considered superfluid, if its evolution actually probes the linear part of the dispersion. Since the longest possible wavelength is equal to the system size, L , we plug the wavevector $k = \pi/L$ into the dispersion relation in Eq. (5) and obtain $(\pi/L)^{-2}\omega^2 = KJ\eta^2 + J^2(\pi/L)^2$. Thus, to see if the linear part of the dispersion is relevant, we have to compute the ratio between two sound velocities, namely, $c^2 = KJ\eta^2$ and $c_0^2 = J^2(\pi/L)^2$. Furthermore, since c^2 is position dependent, we have to average it: $\langle c^2 \rangle = KJ\eta_0^2/2$. It can be concluded that spin superfluidity becomes pronounced when

$$\frac{\langle c^2 \rangle}{c_0^2} = \frac{KJ\langle \eta^2 \rangle}{J^2(\pi/L)^2} = \frac{K\eta_0^2}{2J(\pi/L)^2} > 1. \quad (9)$$

This criterion can be readily evaluated experimentally by observing the evolution of the in-plane angle. In particular, the evolution stops ($\partial_t \theta = 0$) when $KL^2 \langle n_z \rangle^2 / J\pi^2 =$

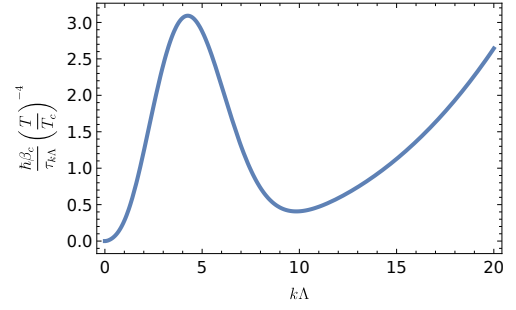


FIG. 3. Typical incoherent dynamics timescale evaluated from the four-magnon interaction term (see the *Supplemental Material* for more details).

1. Therefore, prevalence of spin superfluidity in the sample for large condensate fractions ($\eta_0 > 0.95$) is proven by measuring that $\partial_t \theta > 0$, since $\mathcal{E}[\eta_0^2]$ is a monotonically decreasing function, and since $\langle n_z \rangle^2 (\eta_0 \simeq 0.95) \simeq 1/2$.

Hence, for a large condensate fraction η observing the evolution of θ is sufficient to distinguish between the situation where the critical velocity c vanishes, and where it is substantial. Namely, if $\partial_t \theta < 0$, the system is dominated by quadratic excitations and has a negligible critical velocity, whereas if $\partial_t \theta > 0$, the system displays spin superfluidity. In order to illustrate that our conclusion holds for the full solution for realistic experimental parameters, we plot the numerical solution in Fig. 2.

Incoherent dynamics.— Up to this point we have only considered coherent magnetization dynamics. However, due to nonzero temperatures and interparticle interactions present in real ultracold-atom systems, it is important to consider incoherent (kinetic) processes as well. In particular, it is interesting to study the time scales for the incoherent (kinetic) magnon dynamics and compare them to the time scales for the coherent evolution. We compare these two timescales by evaluating the dominant incoherent timescale set by the four-magnon interaction [48–50] kinetic integral, which we obtain by using the Holstein-Primakoff transformation [40] in order to describe the spin degrees of freedom in this ultracold-atom system in terms of magnons (see *Supplemental Material*). This timescale can be written in the dimensionless form,

$$\frac{\hbar\beta_c}{\tau_{k\Lambda}} = \left(\frac{T}{T_c}\right)^4 I(k\Lambda), \quad (10)$$

where Λ is the thermal magnon de Broglie wavelength, $k_B T_c \simeq 4\pi\hbar J(\rho_m/2.6)^{2/3}$ is the condensation temperature of a noninteracting homogeneous magnon gas with density ρ_m , $\beta = 1/k_B T$ is the inverse thermal energy, and $I(k\Lambda)$ is a dimensionless function, which we evaluate numerically (see Fig. 3). At low momenta, fitting I yields a function $k^2 \log k$, similar to the one reported previously in a field-theoretical calculation [51, 52].

The result of our kinetic theory is the lower bound on the relaxation frequency, since we have only included a single relaxation process. It is likely that due to other

processes (e.g. related to magnetic-field gradients), the relaxation is faster. This statement is consistent with the fact that for a realistic system [53] our result is $1/\tau \simeq 0.2\text{Hz}$, i.e., an order of magnitude lower than the recently reported rate [23]. However, even taking the experimentally reported rate, we see that the coherent dynamics discussed previously is an order of magnitude faster (tens of milliseconds) than the incoherent processes (hundreds of milliseconds). This implies that, while our hydrodynamic description is valid at zero temperature, at finite temperatures the thermal magnons do not equilibrate on the time scales set by the coherent dynamics, which in turn means a hydrodynamic description of the spin dynamics cannot be readily obtained at finite temperature.

This stands in contrast to the situation regarding the scalar degrees of freedom [54] in this system. The difference is mainly due to the different coupling constants, as the four-magnon coupling constant depends on the density and momenta of the magnons, whereas for the scalar degrees of freedom the coupling constant only depends on the s -wave scattering length a of the atom [55]. A typical collision time of atoms in the classical approximation [56] is $\tau_{\text{cl}} = 1/n\sigma v_{\text{rel}}$, where n is the density, $\sigma = 8\pi a^2$ is the collision cross section, and v_{rel} is the relative thermal velocity. For a homogeneous ^{87}Rb gas [57] with a density corresponding to the condensation temperature of $1\mu\text{K}$, at the temperature of $0.1\mu\text{K}$, this collision time is 0.6ms . Therefore, at a nonzero temperature such a system is in the hydrodynamic regime regarding the scalar degrees of freedom, which is enforced by rapid collisions. On the other hand, given the same conditions the magnon dynamics is in the collisionless regime, allowing for far-from-equilibrium states to persist for long periods of time. This timescale hierarchy is well defined, as different timescales are separated by at least one order of magnitude. Finally, the above-described situation concerning magnons in a spinor gas is also different from the binary-mixture situation. There, longitudinal spin kinetics is comparable to the incoherent dynamics of the scalar fields, and hence longitudinal spin currents relax in milliseconds as well [58, 59].

Summary and future work.— In summary, we have examined the zero-temperature coherent dynamics of spinor Bose gases. We have described two experimentally-accessible states illustrating the interplay between superfluidity and spin superfluidity. By evaluating a four-magnon collision integral and comparing the relevant timescales, we have concluded that at nonzero temperatures the magnon gas is in the collisionless regime in stark contrast to the situation concerning the scalar degrees of freedom.

In the future work, we plan to extend our description by including the experimentally-relevant magnetic-field inhomogeneities into our LL equation, which will allow us to make a direct connection to the recent experimen-

tal results on magnon condensation [25, 38]. Another interesting direction is to consider nonzero temperature dynamics of scalar and spin degrees of freedom, which is particularly intriguing in this system due to a clear hierarchy of timescales involved. Finally, we point out that coupling between magnon condensate and thermal cloud is facilitated by the quadratic Zeeman term [60] which could make the experimental control over the build-up of magnon coherence and condensate growth possible. Moreover, this anisotropy will also affect the magnon kinetics.

It is our pleasure to thank Henk Stoof and Gediminas Juzeliūnas for stimulating discussions. J. A. has received funding from the European Union's Horizon 2020 research and innovation programme under the Marie Skłodowska-Curie grant agreement No 706839 (SPINSOCS). R. D. is supported by the Stichting voor Fundamenteel Onderzoek der Materie (FOM), the European Research Council (ERC) and is part of the D-ITP consortium, a program of the Netherlands Organisation for Scientific Research (NWO) that is funded by the Dutch Ministry of Education, Culture and Science (OCW).

* jogundas.armaitis@tfai.vu.lt

- [1] K.-H. Bennemann and J. B. Ketterson, eds., *Novel superfluids*, International Series of Monographs on Physics (Oxford Univ. Press, Oxford, 2013).
- [2] I. M. Khalatnikov, *An Introduction To The Theory of Superfluidity* (Westview Press, 2000).
- [3] C. J. Pethick and H. Smith, *Bose-Einstein Condensation in Dilute Gases; 2nd ed.* (Cambridge Univ. Press, Cambridge, 2008).
- [4] L. A. Sidorenkov, M. K. Tey, R. Grimm, Y.-H. Hou, L. Pitaevskii, and S. Stringari, *Nature* **498**, 78 (2013).
- [5] H. Deng, H. Haug, and Y. Yamamoto, *Rev. Mod. Phys.* **82**, 1489 (2010).
- [6] X.-L. Qi, T. L. Hughes, S. Raghu, and S.-C. Zhang, *Phys. Rev. Lett.* **102**, 187001 (2009).
- [7] D. Tilahun, B. Lee, E. M. Hankiewicz, and A. H. MacDonald, *Phys. Rev. Lett.* **107**, 246401 (2011).
- [8] S. Peotta and P. Törmä, *Nat. Commun.* **6**, 8944 (2015).
- [9] D. J. Dean and M. Hjorth-Jensen, *Rev. Mod. Phys.* **75**, 607 (2003).
- [10] A. Attanasi, A. Cavagna, L. Del Castello, I. Giardina, T. S. Grigera, A. Jelić, S. Melillo, L. Parisi, O. Pohl, E. Shen, and M. Viale, *Nat. Phys.* **10**, 615 (2014).
- [11] E. Sonin, *Adv. Phys.* **59**, 181 (2010).
- [12] S. Takei and Y. Tserkovnyak, *Physical review letters* **112**, 227201 (2014).
- [13] R. A. Duine, A. Brataas, S. A. Bender, and Y. Tserkovnyak, *ArXiv* (2015), arXiv:1505.01329.
- [14] L. J. Cornelissen, J. Liu, R. A. Duine, J. B. Youssef, and B. J. van Wees, *Nat. Phys.* **11**, 1022 (2015).
- [15] A. V. Chumak, V. I. Vasyuchka, A. A. Serga, and B. Hillebrands, *Nat. Phys.* **11**, 453 (2015).
- [16] K. Madison, F. Chevy, W. Wohlleben, and J. Dalibard,

- Phys. Rev. Lett. **84**, 806 (2000).
- [17] O. Marago, S. Hopkins, J. Arlt, E. Hodby, G. Hechenblaikner, and C. Foot, Phys. Rev. Lett. **84**, 2056 (2000).
 - [18] J. R. Abo-Shaeer, C. Raman, J. M. Vogels, and W. Ketterle, Science **292**, 476 (2001).
 - [19] D. M. Stamper-Kurn, M. R. Andrews, A. P. Chikkatur, S. Inouye, H.-J. Miesner, J. Stenger, and W. Ketterle, Phys. Rev. Lett. **80**, 2027 (1998).
 - [20] J. Stenger, S. Inouye, D. M. Stamper-Kurn, H.-J. Miesner, A. P. Chikkatur, and W. Ketterle, Nature **396**, 345 (1998).
 - [21] L. E. Sadler, J. M. Higbie, S. R. Leslie, M. Vengalattore, and D. M. Stamper-Kurn, Nature **443**, 312 (2006).
 - [22] J.-y. Choi, S. Kang, S. W. Seo, W. J. Kwon, and Y.-i. Shin, Phys. Rev. Lett. **111**, 245301 (2013).
 - [23] G. E. Marti, A. MacRae, R. Olf, S. Lourette, F. Fang, and D. M. Stamper-Kurn, Phys. Rev. Lett. **113**, 155302 (2014).
 - [24] R. W. Cherg, V. Gritsev, D. M. Stamper-Kurn, and E. Demler, Phys. Rev. Lett. **100**, 180404 (2008).
 - [25] F. Fang, R. Olf, S. Wu, H. Kadau, and D. M. Stamper-Kurn, ArXiv (2015), arXiv:1511.05193.
 - [26] K. Kudo and Y. Kawaguchi, Physical Review A **84**, 043607 (2011).
 - [27] H. Flayac, H. Terças, D. D. Solnyshkov, and G. Malpuech, Physical Review B **88**, 184503 (2013).
 - [28] Q. Zhu, Q.-f. Sun, and B. Wu, Phys. Rev. A **91**, 023633 (2015).
 - [29] Y. M. Bunkov and G. E. Volovik, J. Phys. Condens. Matter **22**, 164210 (2010).
 - [30] E. Yukawa and M. Ueda, Phys. Rev. A **86**, 063614 (2012).
 - [31] D. M. Stamper-Kurn and M. Ueda, Rev. Mod. Phys. **85**, 1191 (2013).
 - [32] M. Ueda, Annu. Rev. Condens. Matter Phys. **3**, 263 (2012).
 - [33] Y.-T. Oh, P. Kim, J.-H. Park, and J. H. Han, Phys. Rev. Lett. **112**, 160402 (2014).
 - [34] A. Lamacraft, Phys. Rev. A **77**, 063622 (2008).
 - [35] M. Kunimi and H. Saito, Phys. Rev. A **91**, 043624 (2015).
 - [36] J. Armaitis, H. T. C. Stoof, and R. A. Duine, Phys. Rev. Lett. **110**, 260404 (2013).
 - [37] T. Gilbert, IEEE Trans. Magn. **40**, 3443 (2004).
 - [38] R. Olf, F. Fang, G. E. Marti, A. MacRae, and D. M. Stamper-Kurn, Nat. Phys. **11**, 720 (2015).
 - [39] Y. Kawaguchi, H. Saito, and M. Ueda, Phys. Rev. Lett. **98**, 110406 (2007).
 - [40] T. Holstein and H. Primakoff, Phys. Rev. **58**, 1098 (1940).
 - [41] S. O. Demokritov, V. E. Demidov, O. Dzyapko, G. A. Melkov, A. A. Serga, B. Hillebrands, and A. N. Slavin, Nature **443**, 430 (2006).
 - [42] R. E. Troncoso and Á. S. Núñez, Ann. Phys. **346**, 182 (2014).
 - [43] T. Giamarchi, C. Rüegg, and O. Tchernyshyov, Nat. Phys. **4**, 198 (2008).
 - [44] C. Pfleiderer, Rev. Mod. Phys. **81**, 1551 (2009).
 - [45] L. Landau, Phys. Rev. **60**, 356 (1941).
 - [46] A. L. Gaunt, T. F. Schmidutz, I. Gotlibovych, R. P. Smith, and Z. Hadzibabic, Phys. Rev. Lett. **110**, 200406 (2013).
 - [47] D. Niroomand, S. D. Graham, and J. M. McGuirk, Phys. Rev. Lett. **115**, 075302 (2015).
 - [48] F. J. Dyson, Phys. Rev. **102**, 1217 (1956).
 - [49] F. Keffer and R. Loudon, J. Appl. Phys. **32**, S2 (1961).
 - [50] S. P. A.I. Akhiezer, V.G. Bar'yakhtar, JETP **9**, 146 (1959).
 - [51] A. B. Harris, Phys. Rev. **175**, 674 (1968).
 - [52] B. I. Halperin and P. C. Hohenberg, Phys. Rev. **188**, 898 (1969).
 - [53] From Fig. 1 (b) in the paper on coherent magnon optics (Ref. [23]) we read off that $1/\tau \simeq 4\text{Hz}$ for $k = 2\pi/(15.4\mu\text{m})$. No temperature is given in the paper, but assuming that $T = T_c/10$, and taking $T_c \simeq 1\mu\text{K}$ from another paper of the same group (Ref. [38]), we have $k\Lambda \simeq 1/4$ and $\hbar\beta_c \simeq 10^{-5}\text{s}$. These assumptions yield $1/\tau \simeq 0.2\text{Hz}$, which is one magnitude lower than the reported result. Note that it is possible to improve our accuracy by performing an accurate trap average, distinguishing between magnon and gas condensation temperatures and populations etc.
 - [54] H.-J. Miesner, D. M. Stamper-Kurn, M. R. Andrews, D. S. Durfee, S. Inouye, and W. Ketterle, Science **279**, 1005 (1998).
 - [55] A. J. Leggett, Rev. Mod. Phys. **73**, 307 (2001).
 - [56] R. Meppelink, R. van Rooij, J. M. Vogels, and P. van der Straten, Phys. Rev. Lett. **103**, 095301 (2009).
 - [57] M. Egorov, B. Opanchuk, P. Drummond, B. V. Hall, P. Hannaford, and A. I. Sidorov, Phys. Rev. A **87**, 053614 (2013).
 - [58] J. Armaitis, H. T. C. Stoof, and R. A. Duine, Phys. Rev. A **91**, 043641 (2015).
 - [59] S. B. Koller, A. Groot, P. C. Bons, R. A. Duine, H. T. C. Stoof, and P. van der Straten, New J. Phys. **17**, 113026 (2015).
 - [60] B. Flebus, S. A. Bender, Y. Tserkovnyak, and R. A. Duine, (2015), arXiv:1510.05316.

Supplemental material for “Superfluidity and spin superfluidity in spinor Bose gases”

J. Armaitis*

*Institute of Theoretical Physics and Astronomy,
Vilnius University,
A. Goštauto 12, LT-01108 Vilnius, Lithuania*

R. A. Duine

*Institute for Theoretical Physics and Center for Extreme Matter and Emergent Phenomena,
Utrecht University,
Leuvenlaan 4, 3584 CE Utrecht, The Netherlands
(Dated: March 7, 2016)*

This supplemental material file provides (i) an explicit mean-field equation of motion for the atomic fields, (ii) additional details on the four-magnon scattering time calculation, and also (iii) a note concerning the evolution of the order parameter during magnon condensation.

I. MEAN-FIELD EQUATION OF MOTION

In this section we provide the mean-field equation of motion for the atomic fields. The spinor Bose gas is described by the following second-quantized Hamiltonian in terms of the field operators $\hat{\psi}_\mu$ that correspond to atoms with mass M in the hyperfine state μ , also given in the Letter:

$$H = \int d\mathbf{x} \hat{\psi}_\mu^\dagger \left(-\frac{\hbar^2 \nabla^2}{2M} + V(\mathbf{x}) \right) \hat{\psi}_\mu - \hat{\psi}_\mu^\dagger \left(p[\sigma_z]_{\mu\nu} - \hbar K[\sigma_z^2]_{\mu\nu} \right) \hat{\psi}_\nu + (g_0 : \hat{\rho}^2 : + g_1 : \hat{\mathbf{n}}^2 :), \quad (1)$$

where $V(\mathbf{x})$ is the trapping potential, the colons denote normal ordering, g_1 (g_0) is the spin-(in)dependent interaction energy, $\hat{\rho} = \hat{\psi}_\mu^\dagger \hat{\psi}_\mu$ is the density operator, and $\hat{\mathbf{n}} = \hat{\psi}_\mu^\dagger \boldsymbol{\sigma}_{\mu\nu} \hat{\psi}_\nu$ is the local spin operator. For completeness, we note that the mean-field dynamics derived from this Hamiltonian for the fields ψ_μ corresponding to the aforementioned field operators $\hat{\psi}_\mu$ are described by the Gross-Pitaevskii equation,

$$i\hbar \partial_t \psi_\mu = \left(-\frac{\hbar^2}{2M} \nabla^2 + V(\mathbf{x}) - p[\sigma_z]_{\mu\nu} + \hbar K[\sigma_z^2]_{\mu\nu} + g_0 \rho \right) \psi_\mu + g_1 \mathbf{n} \cdot \boldsymbol{\sigma}_{\mu\nu} \rho \psi_\nu. \quad (2)$$

The zero-temperature hydrodynamic equations (3) and (4) in the Letter are obtained from this Gross-Pitaevskii equation.

II. FOUR-MAGNON SCATTERING TIMESCALE

In this section we give additional details concerning the four-magnon scattering time calculation.

Here we consider the exchange term in the spinor Bose gas Hamiltonian, namely, $J : \hat{\boldsymbol{\Omega}} \cdot \nabla^2 \hat{\boldsymbol{\Omega}} :$, where $\hat{\boldsymbol{\Omega}}$ is the full magnetization operator. It can be divided into the magnetization density ρ_s , which we assume to be constant in the deep ferromagnetic regime, and the direction of magnetization operator $\hat{\mathbf{n}}$ in the following way: $\hat{\boldsymbol{\Omega}} = \rho_s \hat{\mathbf{n}}$. Hence, the magnetic excitations only concern the direction of magnetization \mathbf{n} in this regime. For simplicity, we do not consider the quadratic Zeeman effect in this calculation. The Holstein-Primakoff transformation [1, 2] introduces bosonic magnon operators $\hat{b}(\mathbf{k})$, which substitute for the magnetization direction operators. We subsequently perform a semiclassical expansion of these spin fluctuations around the average direction of the magnetization. We retain only two first terms in this large-magnetization expansion.

The lowest-order term yields the kinetic energy for the magnons,

$$\mathcal{H}_2 = \int \frac{d\mathbf{k}}{(2\pi)^3} E_k \hat{b}^\dagger(\mathbf{k}) \hat{b}(\mathbf{k}), \quad (3)$$

* jogundas.armaitis@tfai.vu.lt

where $E_k = \hbar J \mathbf{k}^2$ is the magnon dispersion [3], whereas the subleading term describes the four-magnon interaction,

$$\mathcal{H}_4 = \int \frac{d\mathbf{k}}{(2\pi)^3} \frac{d\mathbf{k}_2}{(2\pi)^3} \frac{d\mathbf{k}_3}{(2\pi)^3} \frac{d\mathbf{k}_4}{(2\pi)^3} \delta^{(3)}(\mathbf{k} + \mathbf{k}_2 - \mathbf{k}_3 - \mathbf{k}_4) g \hat{b}^\dagger(\mathbf{k}) \hat{b}^\dagger(\mathbf{k}_2) \hat{b}(\mathbf{k}_3) \hat{b}(\mathbf{k}_4), \quad (4)$$

where

$$g = \frac{\hbar J}{4\rho_s} (\mathbf{k} \cdot \mathbf{k}_2 + \mathbf{k}_3 \cdot \mathbf{k}_4) \quad (5)$$

is the four-magnon coupling constant. Note that this coupling constant g does not explicitly depend on the scattering properties of the particular atom. From this interaction term, using e.g. the Fermi Golden Rule, we construct a collision integral. The characteristic timescale is thus given by

$$\frac{1}{\tau_{\mathbf{k}}} = \frac{2\pi}{\hbar} \int \frac{d\mathbf{k}_2}{(2\pi)^3} \int \frac{d\mathbf{k}_3}{(2\pi)^3} \int \frac{d\mathbf{k}_4}{(2\pi)^3} g^2 \mathcal{F} \delta(E_{\mathbf{k}} + E_{\mathbf{k}_2} - E_{\mathbf{k}_3} - E_{\mathbf{k}_4}) (2\pi)^3 \delta^{(3)}(\mathbf{k} + \mathbf{k}_2 - \mathbf{k}_3 - \mathbf{k}_4), \quad (6)$$

where

$$\mathcal{F} = f_2(1 + f_3)(1 + f_4) - (1 + f_2)f_3f_4 \quad (7)$$

is a combination of Bose-Einstein distributions $f_i = 1/[\exp(\beta E_{\mathbf{k}_i}) - 1]$, and $\beta = 1/k_B T$ is the inverse thermal energy.

The characteristic-timescale expression in Eq. (6) is subsequently evaluated numerically and yields the result shown in Fig. 3 of the Letter. Note that for small $k\Lambda$, the kinetic frequency $\tau_{k\Lambda}^{-1}$ approaches zero; as $k\Lambda$ increases, $\tau_{k\Lambda}^{-1}$ has a local maximum and a local minimum, and only then does it approach the classical limit. These features can be understood in terms of competition between the Bose enhancement and the four-magnon coupling constant, as the former favors low $k\Lambda$ scattering, while the latter suppresses it.

III. A NOTE ON MAGNON CONDENSATION

In general, during the process of condensate formation, a certain symmetry is broken, leading to a nonzero order parameter. In the case of Bose-Einstein condensation of atoms, the symmetry concerns the phase of the wavefunction, and the order parameter is the average of the atom-annihilation operator. In the condensate of magnons [4, 5], the symmetry concerns the in-plane magnetization angle θ , and the order parameter is related to the out-of-plane magnetization component n_z . It is important to point out that the Landau-Lifshitz equation explicitly preserves the local magnetization $|\mathbf{n}|$ in stark contrast to the dynamics of a BEC of atoms, where no such order-parameter conservation law exists in the grand-canonical description [6]. Therefore, we expect the magnon condensate formation to differ from the process of Bose-Einstein condensation of atoms.

-
- [1] T. Holstein and H. Primakoff, Phys. Rev. **58**, 1098 (1940).
 - [2] A. Auerbach, *Interacting electrons and quantum magnetism* (Springer-Verlag, Berlin, 1994).
 - [3] F. J. Dyson, Phys. Rev. **102**, 1217 (1956).
 - [4] S. O. Demokritov, V. E. Demidov, O. Dzyapko, G. A. Melkov, A. A. Serga, B. Hillebrands, and A. N. Slavin, Nature **443**, 430 (2006).
 - [5] R. E. Troncoso and Á. S. Núñez, Ann. Phys. **346**, 182 (2014).
 - [6] H. Stoof, J. Low Temp. Phys. **114**, 11 (1999).